

Published in final edited form as:

Neuron. 2015 February 4; 85(3): 561–572. doi:10.1016/j.neuron.2014.12.058.

Decreased subcortical cholinergic arousal in focal seizures

Joshua E. Motelow¹, Wei Li^{1,2}, Qiong Zhan^{1,3}, Asht M. Mishra¹, Robert N. S. Sachdev⁴, Geoffrey Liu¹, Abhijeet Gummadavelli¹, Zaina Zayyad¹, Hyun Seung Lee¹, Victoria Chu¹, John P. Andrews¹, Dario J. Englot⁸, Peter Herman^{6,7}, Basavaraju G. Sanganahalli^{6,7}, Fahmeed Hyder^{6,7}, and Hal Blumenfeld^{1,4,5,7}

¹Department of Neurology, Yale University School of Medicine, 333 Cedar Street, New Haven, Connecticut 06520, USA

²Department of Neurosurgery, Jinling Hospital, School of Medicine, Nanjing University, 305 East Zhongshan Road, Nanjing, 210002, Jiangsu Province, People's Republic of China

³Department of Neurology, Xiangya Hospital, Central South University, Changsha, Hunan, 410008, China

⁴Department of Neurobiology, Yale University School of Medicine, 333 Cedar Street, New Haven, Connecticut 06520, USA

⁵Department of Neurosurgery, Yale University School of Medicine, 333 Cedar Street, New Haven, Connecticut 06520, USA

⁶Department of Diagnostic Radiology, Yale University School of Medicine, 333 Cedar Street, New Haven, Connecticut 06520, USA

⁷Core Center for Quantitative Neuroscience with Magnetic Resonance (QNMR) Yale University School of Medicine, 333 Cedar Street, New Haven, Connecticut 06520, USA

⁸Department of Neurological Surgery, University of California - San Francisco, 505 Parnassus Avenue, San Francisco, CA 94143, USA

SUMMARY

Impaired consciousness in temporal lobe seizures has a major negative impact on quality of life. The prevailing view holds that this disorder impairs consciousness by seizure spread to the bilateral temporal lobes. We propose instead that seizures invade subcortical regions and depress arousal, causing impairment through decreases rather than through increases in activity. Using functional magnetic resonance imaging in a rodent model, we found increased activity in regions known to depress cortical function including lateral septum and anterior hypothalamus.

© 2014 Elsevier Inc. All rights reserved.

Correspondence to: Hal Blumenfeld, MD, PhD Yale Depts. Neurology, Neurobiology, Neurosurgery 333 Cedar Street, New Haven, CT 06520-8018 Tel: 203 785-3928 Fax: 203 737-2538 hal.blumenfeld@yale.edu.

Author Contributions J.M., D.E., F.H., and H.B. conceived the experiments. J.M., W.L., Q.Z., A.M., R.S., G.L., A.G., Z.Z., H.L., V.C., P.H., and B.S. performed the experiments. J.M., Z.Z., J.A. and W.L. analyzed the results. J.M. and H.B. wrote the paper.

Publisher's Disclaimer: This is a PDF file of an unedited manuscript that has been accepted for publication. As a service to our customers we are providing this early version of the manuscript. The manuscript will undergo copyediting, typesetting, and review of the resulting proof before it is published in its final citable form. Please note that during the production process errors may be discovered which could affect the content, and all legal disclaimers that apply to the journal pertain.

Importantly, we found suppression of intralaminar thalamic and brainstem arousal systems and suppression of the cortex. At a cellular level, we found reduced firing of identified cholinergic neurons in the brainstem pedunculo-pontine tegmental nucleus and basal forebrain. Finally, we used enzyme-based amperometry to demonstrate reduced cholinergic neurotransmission in both cortex and thalamus. Decreased subcortical arousal is a novel mechanism for loss of consciousness in focal temporal lobe seizures.

Keywords

Acetylcholine; Epilepsy; Sleep; Consciousness; Complex Partial Seizures; Slow-Wave Sleep; Sudden Unexpected Death in Epilepsy; Limbic seizures

INTRODUCTION

Why do patients lose consciousness during temporal lobe seizures? The temporal lobes are not traditionally a part of the consciousness system (Blumenfeld, 2012; Saper et al., 2005); patient HM was conscious without both hippocampi (Scoville and Milner, 1957). Yet in focal temporal lobe seizures, patients often become unresponsive and demonstrate automaton-like behavior (Escueta et al., 1977; Penfield, 1952). During temporal lobe seizures, the cerebral cortex exhibits widespread slow-wave activity interpreted by some as seizure propagation (Lieb et al., 1991). Instead, we propose that these cortical slow oscillations and the coincident reduction in cerebral blood flow represent depressed cortical activity (Blumenfeld et al., 2004a; Blumenfeld et al., 2004b; Englot et al., 2008; Englot et al., 2009; Englot et al., 2010). If true, the subcortical arousal systems should be depressed (Blumenfeld, 2012; Norden and Blumenfeld, 2002) as in other states of unconsciousness such as deep sleep (Steriade et al., 1993b) or coma (Young, 2000).

Reframing impaired consciousness in temporal lobe seizures as a deficit in subcortical arousal leads to several predictions (Figure 1). Increased activity is expected in limbic archicortical structures such as the hippocampus but also in connected subcortical inhibitory regions such as the lateral septal nuclei and anterior hypothalamus, known to project to the subcortical arousal systems (McGinty and Szymusiak, 2001; Mesulam and Mufson, 1984; Varoquaux and Poulain, 1999). Key subcortical arousal regions, such as the brainstem pedunculo-pontine tegmental nucleus (PPT), thalamic intralaminar nuclei (Glenn and Steriade, 1982; Heckers et al., 1992) and the basal forebrain cholinergic nuclei (Mesulam et al., 1983b) are expected to show reduced activity. In addition the release of modulatory arousal neurotransmitters such as acetylcholine should decrease in both cortex (Marrosu et al., 1995) and thalamus (Williams et al., 1994). We previously developed a rodent model which resembles human temporal lobe seizures in terms of electrophysiology and behavioral deficits (Englot et al., 2008; Englot et al., 2009). However to our knowledge, decreased subcortical arousal has not been previously investigated as a mechanism of impairment in epilepsy.

In the present study, we use a combination of high field blood oxygen-level dependent (BOLD) functional magnetic resonance imaging (fMRI), direct electrophysiological recordings, and amperometry-based neurotransmitter measurements to investigate the

modulation of subcortical arousal during limbic seizures on multiple levels. We found that depressed cortical function—evidenced by cortical slow oscillations and decreased fMRI signals—is accompanied by increased activity in the hippocampus, anterior hypothalamus and lateral septum. fMRI signals were decreased in the intralaminar thalamus and midbrain tegmentum, guiding us to perform juxtacellular recordings from the mesopontine cholinergic nuclei, which provide cholinergic excitation of the thalamus (McCormick, 1992; Mesulam et al., 1983b). We found suppressed firing in PPT cholinergic neurons. Further exploring the cholinergic arousal system, we investigated neurons in the cholinergic basal forebrain, which innervate the neocortex (Mesulam et al., 1983a; Rye et al., 1984), and found them suppressed as well. Finally, we showed that choline, as a proxy for acetylcholine, is decreased in both the cortex and thalamus during limbic seizures. Decreased acetylcholine has long been associated with cortical slow oscillations, an inhibited thalamus, and a suppressed basal forebrain in slow-wave sleep (Marrosu et al., 1995; Williams et al., 1994). These data provide direct evidence, for the first time, of seizure activity suppressing subcortical arousal as a mechanism of depressed corticothalamic network function.

RESULTS

fMRI

High field BOLD fMRI revealed a network of cortical and subcortical changes consistent with decreased subcortical arousal in limbic seizures. We conducted fMRI measurements during partial limbic seizures (10 animals, 34 seizures, mean duration \pm SEM 70.72 ± 4.01 seconds), induced by brief hippocampal stimulation (Englot et al., 2008; Englot et al., 2009). A quadrature coil design (Hyde et al., 1987) improved the detection power of our fMRI recordings in critical ventral subcortical areas not visualized previously during seizures (Englot et al., 2008; Englot et al., 2009).

We found decreased cortical fMRI activity paired with both subcortical increases and decreases during partial limbic seizures (Figures 2 and 3). BOLD increases were found in the hippocampus, hypothalamus, and septum while decreases were seen in the cortex, intralaminar thalamus, and midbrain tegmentum. Guided by the fMRI t-map results (Figure 2), we targeted six regions of interest (ROI) (Figure 3A) to investigate changes over time. Three of the ROIs, namely hippocampus (HC), septum, and anterior hypothalamus (Ant Hyp), showed prominent BOLD fMRI increases followed by postictal decline and eventually a return to baseline (Figure 3B). These regions all show increased multiunit activity ictally with rapid decrease postictally (Figure S1) suggesting that the slow decay of the BOLD signal in these regions postictally may represent perfusion decreasing more slowly than neural activity (Hyder et al., 2010). All three regions showed significant increases during seizures compared to baseline (Figure 3C) (comparing seizure to baseline: HC $+3.63\% \pm 0.40\%$, Septum $+3.04\% \pm 0.53\%$; Ant Hyp $+2.06\% \pm 0.28\%$; 1-sample t-tests Holm-Bonferroni corrected, $P < 0.05$). The hypothalamus plays a key role in promoting slow-wave sleep (Saper et al., 2005), and stimulation of both the lateral septum (Englot et al., 2009) and anterior hypothalamus (Sterman and Clemente, 1962) causes cortical slow oscillations resembling deep sleep. These changes are therefore consistent with a model in

which loss of consciousness during partial seizures is caused by increased activity in inhibitory projection areas (Figure 1).

Three ROIs were chosen to investigate BOLD decreases (Figure 3A). We have previously reported BOLD decreases in the lateral orbital frontal cortex (LO), which is consistent with decreased metabolic activity associated with ictal neocortical slow activity (Blumenfeld et al., 2004a; Englot et al., 2008; Englot et al., 2009; Englot et al., 2010). In addition, two major subcortical arousal areas were chosen, the intralaminar central lateral thalamus (CL) and midbrain tegmentum (MT). The BOLD signal in these three ROIs decreased during partial seizures, remained suppressed postictally, and then gradually returned to baseline (Figure 3B). The orbital frontal cortex, intralaminar thalamus, and midbrain tegmentum all showed significant fMRI decreases during seizures compared to baseline (Figure 3C) (comparing seizure to baseline: LO $-3.65\% \pm 0.61\%$; CL $-0.93\% \pm 0.30\%$; MT $-1.07\% \pm -0.27\%$; 1-sample t-tests Holm-Bonferroni corrected, $P < 0.05$). The brainstem tegmentum is comprised of arousal nuclei including the major source of cholinergic input for the intralaminar thalamus (Hallanger et al., 1987; Mesulam et al., 1983b). This circuit is vital for promoting the excitatory actions of the thalamus on cortex and for maintaining thalamic neurons in their regular firing mode (Glenn and Steriade, 1982; McCormick, 1992). The thalamus and midbrain tegmentum have long been implicated in arousal, working both cooperatively and independently (Glenn and Steriade, 1982; Hallanger et al., 1987; Mesulam et al., 1983b; Moruzzi and Magoun, 1949; Poulet et al., 2012; Steriade et al., 1993a).

PPT Juxtacellular recordings

Our BOLD data showed decreased signal across both the midbrain tegmentum and intralaminar thalamus (Figures 2 and 3). The arousal-promoting brainstem cholinergic system located in the brainstem tegmentum, centered in the PPT, provides a physiological bridge between the two anatomical regions (Steriade et al., 1993a). Acetylcholine originating from the brainstem has a profound direct effect on the thalamus (McCormick, 1992) and therefore serves as an indirect vehicle of cortical arousal (Moruzzi and Magoun, 1949; Steriade et al., 1993a). The PPT is a heterogeneous nucleus although the non-cholinergic neurons also have a putative arousal role via the forebrain cholinergic system (Steriade et al., 1993a). To determine whether the brainstem cholinergic system is truly suppressed during limbic seizures, we conducted juxtacellular recordings in the PPT. Locations of all identified neurons recorded in the PPT and peri-PPT region are in Figure S2.

A representative recording from a cholinergic neuron is shown (Figure 4). The neuron fired regularly prior to seizure initiation (Figure 4A, Baseline). During the seizure in the hippocampus (Figure 4A, Seizure), the cortical multiunit activity (MUA) converted to Up and Down states (Steriade et al., 1993b) of alternating firing and quiescence while the cortical local field potential (LFP) converted to prominent slow oscillations as described previously (Englot et al., 2008). At the same time, the cholinergic neuron markedly decreased its firing almost immediately after the seizure begins. In the postictal period (Figure 4A, Postictal), the cortical LFP was still dominated by low-frequency oscillations,

and the cholinergic neuron remained depressed, but its firing rate later began to recover. After a few minutes, the animal recovered back to baseline (Figure 4A, Recovery). The cortical LFP was again dominated by higher frequency activity resembling wakefulness, and the cholinergic neuron again fired regularly. The neuron recorded here, which co-stained for choline acetyltransferase, can be seen in Figure 4B.

Identified cholinergic neurons as a group displayed a consistent and dramatic decrease in firing during seizures (see Figures 6A and 6B) (8 neurons from 8 animals; mean seizure duration: 60.34 seconds \pm 6.22 seconds; comparing seizure to baseline: mean change in firing rate -2.31 Hz \pm 0.71 Hz; paired t-test Holm-Bonferroni corrected, $P < 0.05$). Although they possessed variable firing rates at baseline, all cholinergic neurons decreased their firing rates during seizures. The firing rates slowly recovered during the post ictal period and resumed normal firing after a variable interval. All cholinergic neurons fired tonically and relatively slowly. None exhibited burst firing.

The non-cholinergic neurons in the PPT region are predominately glutamatergic and GABAergic (Wang and Morales, 2009). The putative arousal-promoting role of the glutamatergic neurons entails exciting the cholinergic basal forebrain (Steriade et al., 1993a). We did not distinguish between the two cell types in this study but found that unlike cholinergic neurons, which consistently decreased their firing during seizures, non-cholinergic neurons showed mixed behaviors including decreased, increased or no change in firing rates. An example recording from a non-cholinergic PPT neuron is shown in Figure S3, with no appreciable change in firing during a partial seizure. Overall, the mixture of increased, decreased or no change in firing rate of noncholinergic neurons during the seizure period led to no significant change from baseline on average (see Figures 6E and 6F) (21 neurons from 19 animals; mean seizure duration: 62.19 seconds \pm 5.42 seconds; comparing seizure to baseline: mean change in firing rate +1.04 Hz \pm 3.45 Hz; paired t-test, $P = 0.76$). We observed that some noncholinergic neurons began firing in bursts during seizures (Figure S4), which accounts for the apparent rise in mean firing rate in the late ictal period (Figure 6F). The non-bursting neurons trended towards decreased firing (Figures S4AD and S4E) (13 cells; mean seizure duration 61.11 seconds \pm 7.06 seconds; comparing seizure to baseline: mean change in firing rate -2.44 Hz \pm 1.17 Hz; paired t-test, $P = 0.06$) while the bursting neurons trended towards increased firing (Figures S4F and S4G) (8 cells; mean seizure duration 63.93 seconds \pm 9.00 seconds; comparing seizure to baseline: mean change in firing rate +6.71 Hz \pm 8.84 Hz; paired t-test, $P = 0.47$).

In order to get a more complete picture of the overall regional activity within and around the pedunculopontine tegmental nucleus, we also analyzed the single cell juxtacellular recordings in the population of neurons in which the electrode tract approached the PPT but the specific recorded cell could not be recovered histologically. The change in firing of these neurons during seizures was significantly decreased (Figures S4H and S4I) (33 neurons from 19 animals: mean seizure duration 54.73 seconds \pm 6.22 seconds; comparing seizure to baseline: mean change in firing rate -3.44 Hz \pm 0.72 Hz; paired t-test Holm-Bonferroni corrected, $P < 0.05$). The overall decrease in firing rate of cells in this region was consistent with decreased BOLD signal (Figure 2) in the brainstem tegmentum during seizures.

Basal forebrain juxtacellular recordings

While the cholinergic neurons in PPT indirectly activate the cortex, the cholinergic neurons of the basal forebrain project directly to neocortex (Mesulam et al., 1983a; Rye et al., 1984), and acetylcholine has a profound effect on state changes in the cortex (Kalmbach et al., 2012; Metherate and Ashe, 1991; Metherate et al., 1992). Like PPT, the cholinergic neurons in the basal forebrain are intermingled with noncholinergic cells although these neurons may have arousal promoting effects as well (Freund and Meskenaite, 1992). Given the suppression of the brainstem cholinergic system, the presence of cortical slow-waves, and the increased activity in slow-wave sleep-promoting regions on fMRI (Figure 2), we extended our juxtacellular recordings to the basal forebrain. Locations of all identified neurons recorded in the basal forebrain are in Figure S5.

A representative recording from a cholinergic neuron in basal forebrain is shown (Figure 5). The neuron fires tonically at baseline (Figure 5A, Baseline), decreases during the seizure (Figure 5B, Seizure), remains suppressed postictally (Figure 5A, Postictal), and eventually returns to baseline (Figure 5A, Recovery). As in the example shown for the PPT neuron (Figure 4), the cortical LFP shows high-frequency low-voltage activity associated with MUA tonic firing at baseline (Figure 5A, Baseline). During the seizure, the cortical LFP converts to low-frequency high-voltage oscillations associated with Up and Down states in MUA (Figure 5A, Seizure). The depressed cortical state persists postictally (Figure 5A, Postictal) and then returns to its baseline state (Figure 5A, Recovery). The neuron recorded here, which co-stained for choline acetyltransferase, can be seen in Figure 5B.

Identified cholinergic neurons in basal forebrain consistently decreased their firing during seizures (Figure 6C and 6D) (7 neurons from 6 animals; mean seizure duration: 77.21 seconds \pm 16.17 seconds; comparing seizure to baseline: mean change in firing rate -4.36 Hz \pm 1.01 Hz; paired t-test Holm-Bonferroni corrected, $P < 0.05$). All cholinergic neurons decreased firing during seizures.

As in PPT, non-cholinergic neurons in the basal forebrain are predominantly glutamatergic and parvalbumin- and neuropeptide Y-containing GABA neurons (Brashear et al., 1986; Duque et al., 2007). The GABAergic neurons may promote arousal by inhibiting cortical interneurons (Freund and Meskenaite, 1992) although both GABAergic and glutamatergic neurons have varied relationships to the cortical EEG and to sleep-wake cycles; some neurons are correlated with wakefulness and dysynchronous EEG and some are not (Hassani et al., 2009). As we did with PPT non-cholinergic neurons, we did not distinguish between the two cell types in the basal forebrain. Unlike basal forebrain cholinergic neurons, which consistently decreased their firing during seizures, non-cholinergic neurons showed mixed behaviors during seizures. An example recording from a non-cholinergic basal forebrain neuron, which increases its firing rate, is shown in Figure S6. Overall, the mixture of increased, decreased, or no change in firing rate of non-cholinergic neurons during the seizure period, led to a non-significant decrease in firing during seizures (Figures 6G and 6H) (18 neurons from 12 animals; mean seizure duration: 86.61 seconds \pm 10.16 seconds; comparing seizure to baseline: mean change in firing rate -1.97 Hz \pm 1.71 Hz; paired t-test, uncorrected $P = 0.4$).

The temporal relationship between single neuron firing and low-frequency oscillations in the cortex is displayed in Figure S7. Cortical LFP 1-4 Hz power increases during seizures and decreases slowly postictally (Figure S7A). In contrast, cholinergic neurons in PPT (Figure S7B) and basal forebrain (Figure S7C) decrease firing during seizures and rise back to baseline postictally. Non-cholinergic neurons in the PPT (Figure S7D) and basal forebrain (Figure S7E) had inconsistent relationship to cortical LFP.

Choline recordings

To study the relationship between acetylcholinergic neurotransmission and ictal neocortical slowing, we measured choline levels using high-temporal resolution amperometry (Parikh et al., 2004). Traditional methods of measuring neurotransmitters such as microdialysis suffer from low temporal resolution, making detection of transient changes during seizures challenging (Marrosu et al., 1995; Parikh et al., 2004). Enzyme-based amperometry allowed us to measure choline levels as a proxy for extracellular acetylcholine with sub-second timing (Burmeister and Gerhardt, 2003; Parikh et al., 2004). Cortical acetylcholine originates primarily from the basal forebrain (Rye et al., 1984) while thalamic acetylcholine originates from the brainstem cholinergic nuclei (Hallanger et al., 1987).

We have already demonstrated direct evidence of suppressed firing in brainstem and basal forebrain cholinergic neurons (Figures 4, 5, 6A, 6B, 6E, and 6F). To confirm that acetylcholine levels were in fact suppressed in arousal-related target areas of these nuclei, we measured cortical and thalamic levels of choline. An example choline recording from the orbital frontal cortex is shown (Figure 7A). Choline recordings in the orbital frontal cortex during limbic seizures revealed choline decreases during seizures that persisted postictally and eventually returned to baseline (Figure 7A). After a stimulus artifact, which caused increased signal in all 4 electrodes, the choline oxidase-coated electrodes showed decreased signal during the seizure. At the same time, the sentinel electrodes returned to baseline following the stimulus artifact. Subtraction of these recordings provided the self-referenced choline signal, which reveals decreased choline during the seizure and gradual recovery back to baseline postictally. Simultaneous recordings of the hippocampal and cortical LFP showed cortical slow oscillations during the seizure and postictal period followed by normal cortical fast activity after recovery (Figure 7B and lower insets).

On a group level, choline decreased significantly in the cortex during partial seizures (Figures 8A and 8C) (10 seizures from 6 animals; mean seizure duration 68.21 seconds \pm 6.26 seconds, comparing seizure to baseline: mean choline concentration change $-0.086 \mu\text{M} \pm 0.032 \mu\text{M}$; paired t-test Holm-Bonferroni corrected, $P < 0.05$). A similar picture was seen in CL, an important target of brainstem cholinergic neurons in the intralaminar thalamus. The thalamic choline signal decreased during partial seizures (Figures 8B and 8C) (7 seizures from 5 animals; mean seizure duration 53.11 seconds \pm 5.51 seconds, comparing seizure to baseline: mean choline concentration change $-0.031 \mu\text{M} \pm 0.009 \mu\text{M}$; paired t-test Holm-Bonferroni corrected, $P < 0.05$). The signal declined during the seizures and then began to return to baseline levels as the animals recovered in both cortex (Figure 8A) and thalamus (Figure 8B). This reflects suppression of the cholinergic neurotransmission arising

from basal forebrain (Figures 5, 6C and 6D) and pedunculopontine tegmental nucleus (Figures 4, 6A, and 6B), respectively.

To further confirm the validity of our measurements, cholinergic transmission was also evaluated using a stimulus known to produce increased (rather than decreased) physiological arousal. At the end of the recording session, the animals were put back into deep anesthesia and toe pinch was administered to evaluate the cholinergic response. Toe pinch is known to increase firing in cholinergic PPT neurons as well as activate cortex (Mena-Segovia et al., 2008). Toe pinch caused significant choline increases in both cortex (9 animals; comparing seizure to baseline: mean choline concentration change $+0.122 \mu\text{M} \pm 0.032 \mu\text{M}$; paired t-test Holm-Bonferroni corrected, $P < 0.05$) and thalamus (8 animals; comparing seizure to baseline: mean choline concentration change $+0.040 \mu\text{M} \pm 0.014 \mu\text{M}$; paired t-test Holm-Bonferroni corrected, $P < 0.05$) (Figure 8C).

DISCUSSION

The prevailing view holds that deficits during seizures are caused by sudden abnormal or excessive activation of cortical circuits. Our data present a very different mechanism for impaired cortical function, demonstrating that subcortical arousal circuits show markedly decreased activity in limbic seizures associated with a depressed cortex resembling deep sleep or coma. Our data identify, for the first time, suppression of subcortical arousal systems during partial limbic seizures. Suppressed cholinergic and other subcortical arousal is a mechanism consistent with the “network inhibition hypothesis” (Figure 1) for loss of consciousness during complex partial temporal lobe seizures (Blumenfeld, 2012; Norden and Blumenfeld, 2002). We have presented data in which a partial seizure drives a transition from an “aroused” state characterized by “fast” cortical LFP into a “depressed” state marked by cortical slow-waves and decreased fMRI signals in the cortex, thalamus, and brainstem (Figures 2 and 3). Given the role of cholinergic neurons in providing excitatory input to the intralaminar thalamus and cortex (Steriade, 2004), we recorded from identified neurons in the brainstem and basal forebrain. In agreement with our hypothesis, firing of cholinergic neurons in both nuclei was consistently suppressed (Figures 4, 5 and 6). To study effects on cholinergic output to cortex and thalamus we measured choline levels and found decreases in both the intralaminar thalamus and cortex during partial seizures (Figures 7 and 8). Overall these coordinated changes provide strong evidence for reduced subcortical arousal during partial seizures.

Our data reveal a mechanism underlying loss of consciousness during partial seizures that mimics elements of slow-wave sleep. The ictal slow oscillation has similar properties to the slow oscillation of slow-wave sleep and is likely precipitated by similar factors. In both slow-wave sleep and ictal slow oscillations, low-frequency activity dominates the EEG, and Up and Down states are seen in the MUA. In slow-wave sleep, this is thought to be facilitated by decreased firing of subcortical arousal neurons and decreased arousal neuromodulators such as acetylcholine in the cortex and thalamus (Marrosu et al., 1995; McCormick and Bal, 1997), and our data revealed a similar mechanism in partial seizures. Finally, slow-wave sleep is also marked by decreased acetylcholine in the thalamus (Williams et al., 1994), which also occurred in partial seizures. Activity changes in cortex,

thalamus, and brainstem are prominent during anesthesia (Langsjo et al., 2012) and slow-wave sleep (Braun et al., 1997) induction. Consistent with a broad suppression of the arousal system, patients with temporal lobe and other partial seizures demonstrate a bimodal distribution with respect to impairment of consciousness (Cunningham et al., 2014). In most patients, consciousness is either fully impaired or fully intact, which suggests an overall decrease in the level of consciousness rather than impairment of selected contents of consciousness (Posner et al., 2007). These observations provide a human behavioral correlate for the present findings of depressed arousal mechanisms during seizures.

The arousal system is complex, consisting of at least seven potential parallel pathways of cortical and subcortical excitation (Saper et al., 2005). Our experiments demonstrate a strong correlation between cortical depression and a depressed cholinergic system during partial seizures. The current experiments do not determine whether the decrease in cholinergic transmission causes cortical depression. However, optogenetic stimulation of cholinergic PPT neurons decreases cortical slow-wave activity during partial seizures (Furman M, et al., “Optogenetic stimulation of cholinergic mesopontine neurons for preventing cortical dysfunction during seizures” Society for Neuroscience 2013, Poster #53.19/U12), and electrical stimulation of cholinergic targets in the intralaminar thalamic CL reduces seizure-associated cortical slowing and promotes behavioral arousal (Gummadavelli et al., In press). Although cholinergic systems play an important role in arousal, it is likely that suppression of other subcortical arousal systems also participate in loss of consciousness during seizures. Future studies are needed to determine the role of other candidates such as noradrenergic neurons in the locus coeruleus, serotonergic neurons in the raphe and orexin neurons in the lateral hypothalamus.

Additional work is needed to explore the mechanism behind the suppressed neuronal activity in the subcortical arousal systems during seizures. It is possible that excitatory input to these systems has been removed or that inhibitory input has been increased. Initial evidence suggests that increased inhibitory inputs to subcortical arousal systems may play a role, including the following: 1) lateral septum and anterior hypothalamus show large BOLD increases (Figures 2 and 3) during seizures. These regions are known to contain GABAergic neurons with inhibitory projections to subcortical arousal systems (McGinty and Szymusiak, 2001; Mesulam and Mufson, 1984; Saper et al., 2005; Semba and Fibiger, 1992; Varoquaux and Poulain, 1999). 2) Disconnection of excitatory inputs to these inhibitory structures by cutting the fornix prevents ictal cortical slow activity and prevents behavioral arrest (Englot et al., 2009). 3) Electrical stimulation of the lateral septal nuclei or anterior hypothalamus reproduces cortical slow-wave activity and behavioral arrest (Englot et al., 2009; Serman and Clemente, 1962). Future studies are needed to investigate the potential role of descending inhibition in decreased subcortical arousal during and following partial seizures.

Low-frequency oscillations persist postictally (Figure 4A and 5A, **Postictal**) as they do in epilepsy patients (Blumenfeld et al., 2004b; Englot et al., 2010), but the mechanism causing a “depressed” state in the cortex is likely different from the mechanism during the ictal period. We have hypothesized that arousal systems are suppressed during partial seizures because seizure activity leads to increased inhibition in the subcortical arousal systems.

Support for this hypothesis has come from fornix transection that prevents ictal slow-waves, and lateral septal stimulation that can reproduce slow-waves (Englot et al., 2009). However, postictal firing in the hippocampus, lateral septum, and anterior hypothalamus are suppressed rather than hyperactive (Figure S1) suggesting a different mechanism for postictal slow-waves. The BOLD signal in these regions does remain elevated in the initial postictal period (Figure 3B, Postictal) despite suppressed MUA activity (Figure S1), but this is likely related to a slower decay in perfusion relative to neural activity. Because we have observed gradual recovery of cholinergic firing in parallel with decreasing slow-waves in the postictal period (Figure S7A, S7B and S7C) we can speculate that persistent depression of subcortical arousal may still contribute. However, future studies will be needed to fully determine the mechanisms of depressed arousal and low-frequency oscillations in the postictal period.

Impaired consciousness in partial seizures has a major negative impact on quality of life in people with epilepsy, causing unsafe driving, impaired work and school performance, and social stigmatization (Sperling, 2004). In addition, impaired arousal in the postictal could contribute to difficulty in protecting the airway in patients found with their face blocked by a pillow causing sudden unexpected death in epilepsy (SUDEP) (Kloster and Engelskjøn, 1999). Although stopping seizures is the best way to prevent these negative consequences, converting focal seizures with impaired consciousness to focal seizures without impaired consciousness would greatly benefit patients with refractory epilepsy. The findings presented here point to new potential therapeutic avenues to increase subcortical arousal during and following seizures, including electrical and optogenetic deep brain stimulation and targeted pharmacological interventions to improve level of consciousness.

Large-scale network switching in the brain is an important emerging area of neuroscience research. Understanding the mechanisms underlying network switching in seizures may have implications for understanding normal transitions seen in sleep (Saper et al., 2010) and in reciprocal task-positive and default-mode networks (Fox et al., 2005). We have found converging evidence based on fMRI mapping, juxtacellular recordings from brainstem neurons, and electrochemical transmitter measurements that partial limbic seizures lead to depressed subcortical cholinergic arousal, which may play a critical role in loss of consciousness. We propose a paradigm shift for studying and treating partial seizures in which loss of consciousness is understood as a decrease in subcortical arousal and a sudden transition into a state resembling slow-wave sleep.

EXPERIMENTAL PROCEDURES

For full details of experimental procedures see Supplemental Experimental Procedures online.

Animal preparation and surgery

All procedures were conducted in full compliance with approved institutional animal care and use protocols. A total of 138 adult female Sprague Dawley rats (Charles River Laboratories) weighing 202-365 gram were used in these experiments. All surgeries were performed under deep anesthesia with ketamine (90 mg/kg) and xylazine (15 mg/kg). After

surgery animals used in fMRI experiments were allowed at least 6 days of recovery prior to imaging (see below) whereas animals for juxtacellular and neurotransmitter experiments were switched to a low-dose, “light-anesthesia” ketamine (40 mg/kg) and xylazine (7 mg/kg) for immediate recordings as described previously (Englot et al., 2008). All stereotactic coordinates were taken from Paxinos and Watson (Paxinos and Watson, 1998) and were measured in millimeters relative to bregma. Following experiments, animals were sacrificed with Euthasol (Virbac), and brains were harvested for histological analysis and to verify electrode locations.

fMRI experiments

Our implant and imaging methods have been described previously (Englot et al., 2008). In brief, at least 6 days before fMRI recordings, animals were implanted stereotactically with an MRI-compatible bipolar tungsten electrode in the right dorsal hippocampus. To record scalp electroencephalogram (EEG) simultaneously with fMRI, a pair of carbon fiber electrodes were placed bilaterally over the cortex between the scalp and the skull on the day of the experiment. After surgery and preparation for fMRI experiments, animals were switched to a low-dose ketamine/xylazine and maintained under this light anesthesia regimen during seizure induction as described previously (Englot et al., 2008; Englot et al., 2009). fMRI recordings were acquired on a modified 9.4 T system with Varian spectrometer using a custom-built 2×1 ^1H surface quadrature coil for transmitting and receiving radio frequency pulses (Hyde et al., 1987). High spatial resolution anatomical images were acquired with 10 slices in the coronal plane using gradient-echo or spin-echo contrast. For fMRI, a single shot spin echo-planar imaging (SE-EPI) sequence was used: TR, 1000 ms; TE, 25 ms; FOV, 25×25 mm; matrix, 64×64 ; in-plane resolution, 390×390 μm ; contiguous slices of 1 mm, with 10 slices obtained in the same planes as anatomical images. The fMRI images were obtained with 1 s acquisition followed by 2 s delay to enable EEG and LFP signals to be readily interpreted during imaging (Englot et al., 2008; Mishra et al., 2011; Schridde et al., 2008). 200 acquisitions (150 acquisitions in one animal) were acquired per 600-second experiment. Partial seizures were induced approximately 1 minute following the beginning of BOLD acquisitions.

Partial seizures were induced approximately 1 minute following the beginning of BOLD acquisitions as described previously (Englot et al., 2008; Englot et al., 2009) with a 2 s stimulus train delivered between the bipolar hippocampal contacts consisting of square wave biphasic (1 ms per phase) pulses at 60 Hz.

fMRI analysis

Group t-map—Image analysis was completed using statistical parametric mapping (SPM8, <http://www.fil.ion.ucl.ac.uk/spm/>) and in-house software written in Matlab (R2009a, MathWorks, Inc.). Baseline was defined by the mean of 10 images just prior to each seizure. For each seizure, mean ictal percent change images were calculated using all images from the seizure compared to baseline. If an animal had more than one seizure, a mean ictal percent change image was calculated for that animal by taking the mean image across seizures. A 1-sample t-test was then performed on the co-registered percent-change maps

using SPM8. A false discovery rate (FDR) corrected P -value of 0.05 was used for thresholding.

Time courses—For each animal, regions of interest (ROI) were drawn on its high-resolution anatomical image using a rat-brain atlas (Paxinos and Watson, 1998). Signals were obtained using bilateral ROIs except for in the case of the hippocampus and intralaminar thalamic CL in which only the left side (contralateral to the electrode) was used due to hippocampal electrode imaging artifact in the right ROI (e.g., Figures 2 AP slices -3.4 mm and -4.4 mm and 3A). BOLD signal changes in each ROI were computed as a percent change of the ROI's baseline values. Baseline data included 30 seconds prior to seizure onset. Seizure data included the entire timecourse of the seizure scaled to mean seizure duration to allow for averaging across animals. Postictal data were aligned to seizure offset without scaling (Figure 3B). A 1-sample two-tailed t -test was computed for each ROI using the mean ROI percent change during the ictal acquisitions. Significance threshold was $P < 0.05$ with Holm-Bonferroni correction.

Acute LFP, MUA, juxtacellular and choline animal preparation

A bipolar electrode for stimulating/recording LFP was stereotactically placed in the left dorsal hippocampus. In juxtacellular recordings, a high impedance monopolar electrode for recording local field potential (LFP) and multiunit activity (MUA) was implanted into the right lateral orbital frontal cortex (LO) (AP, +4.2; ML, 2.2; SI, 2.4). In choline recordings to avoid shunting amperometry signals via the ground, instead of a high impedance MUA/LFP electrode we used a bipolar LFP electrode for recordings from LO.

Juxtacellular recordings

Data acquisition—Extracellular single unit recordings were acquired using the juxtacellular method (Pinault, 1996). 1.5 mm glass capillaries were filled with 4% Neurobiotin (Vector Laboratories, SP-1120) in saline. The pedunclopontine tegmental nucleus was targeted at coordinates (AP, -7.8; ML, 2.0; SI, 7.0) and basal forebrain recordings were targeted at coordinates (AP, 0.7; ML, 2.8; SI, 7) using a micromanipulator (Sutter Instruments). Juxtacellular recordings were acquired on an Axoclamp-2B amplifier. Seizures were induced as described above for fMRI experiments. Once seizure activity was recorded and the animal returned to baseline, neurons were labeled as described previously (Ros et al., 2009).

Juxtacellular analysis—Spike sorting on the juxtacellular recordings was performed using Spike2 (CED, v5.20a) and recordings were analyzed using in-house software written on Matlab. Firing rate analyses for each group (cholinergic, non-cholinergic, unrecovered) were performed using paired two-tailed t -tests comparing the firing rate for 30 seconds prior to seizure initiation with the firing rate during the seizure. Significance threshold was $P < 0.05$ Holm-Bonferroni corrected. Mean changes in firing rates are graphed and reported \pm SEM. “Bursting cells” are those which have ≥ 1 burst during the recording session. A burst is defined as ≥ 1 interspike interval ≤ 10 ms (Ushimaru et al., 2012).

Immunohistochemistry

Tissue preparation

Following juxtacellular recordings, rats were perfused with heparinized saline followed by 4% paraformaldehyde and brains were post-fixed for 24-48 hours. The brainstem was cut using a Leica Vibratome (Leica, Inc. VT1000S), and slices were incubated in cyanine 3-conjugated to streptavidin. Slices were inspected for Neurobiotin filled cells. The slices containing the cell bodies were incubated overnight in goat- α -choline acetyltransferase (Millipore, 1:500) and then for 1 hour in secondary (Alexa Fluor 647, donkey α -goat).

Microscopy

Slices were “wet mounted” in order to locate the individual slice containing the labeled cell. These cells were visualized on a Zeiss Axiophot microscope with AxioCam HRc and AxioVision software. Confocal images were taken on a Zeiss LSM 710 Duo NLO/multiphoton microscope using a C-Apochromat 63x/1.2 W Corr objective. Additional microscopy was performed on a DM5500 from Leica Microsystems.

Amperometry recordings Data acquisition

Choline measurements were performed using choline-oxidase enzyme coated amperometric biosensors (Quanteon) on a FAST system (FAST16- mkI, Quanteon). Electrodes were ceramic-based microelectrodes with 4 rectangular ($15 \times 333 \mu\text{m}$) platinum recording sites in side-by-side pairs (S2, Quanteon). Electrodes were purchased uncoated and prepared with choline oxidase enzyme coating in-house per the manufacturer’s instructions. Electrode preparation is described in greater detail elsewhere (Parikh et al., 2004).

After *m*-PD plating, electrodes were calibrated *in vitro* (Figure S8) before the experiment using fixed potential amperometry. After a stable baseline was achieved (~30 minutes), aliquots of AA, choline, and DA were added to achieve final concentrations of $250 \mu\text{M}$ AA; 20, 40, and $60 \mu\text{M}$ choline, and $2 \mu\text{M}$ (DA). Only electrodes passing the following inclusion criteria were included: sensitivity for detecting choline on the coated electrodes, $> 5 \text{ pA}/\mu\text{M}$; limit of detection (LOD) for choline, $< 350 \text{ nM}$; ratio of selectivity for choline and AA, $> 180:1$; linearity of coated electrodes response to increasing analyte concentrations ($20\text{-}60 \mu\text{M}$), Pearson’s correlation coefficient (R^2) > 0.99 .

Once the electrodes were placed a few hundred μm s above the target in the left orbital frontal cortex or thalamic intralaminar CL (AP, -2.5 ; ML, 1.5 ; SI, 4.7), the electrodes were lowered to locate “pockets” of fluctuations in choline signal suggesting the presence of cholinergic terminals in the cortex or thalamus. If the choline signal increased after lowering, the signal was allowed to return to baseline before seizures were initiated, using the same methods as in juxtacellular experiments. At the conclusion of the experiment, animals were deeply anesthetized and toe pinches were administered to activate cholinergic arousal (Mena-Segovia et al., 2008; Zhang et al., 2009).

Choline data analysis—*In vitro* calibration criteria above were used to determine which coated electrodes were used for recordings. Sentinel electrodes were excluded if they malfunctioned during the transfer between *in vitro* beaker calibration and *in vivo* recordings.

All signals were first smoothed by subtracting a 10-point moving average. Low-frequency “drift” was removed by subtracting a 400-point moving average. Large artifacts (such as the occasional artifact generated by electrical stimulus to the hippocampus) were removed from the signal to prevent unwanted effects to the drift removal. The first 12.5 seconds of seizure activity were removed for both display and statistical purposes to remove artifact generated by the 2-second hippocampal stimulus. Statistical analyses were performed for each group (partial seizures and toe pinch). The mean choline concentration during 30 seconds of baseline were compared to the mean choline concentration during seizures (after discarding the first 12.5 seconds) or toe pinch (after discarding the first 25 seconds to allow for steady state). A paired two-tailed t-test was performed for each group to determine change from baseline. Holm-Bonferonni correction was used to account for multiple comparisons first for the seizure groups and then separately for the toe pinch groups, with corrected significance threshold $P < 0.05$. Mean changes in concentrations are graphed and reported \pm SEM.

Supplementary Material

Refer to Web version on PubMed Central for supplementary material.

Acknowledgements

We thank Moran Furman for helpful discussions. We thank Vinay Parikh for advice and Quanteon LLC for technical support for the amperometry measurements. We thank Alvaro Duque, Al Mennone and William Cafferty for their microscopy assistance. This work was supported by NIH R01 NS066974, the Swebelius Fund, and the Betsy and Jonathan Blattmachr Family (HB); NIH P30 NS052519 (FH); NIH F30 NS071628 and MSTP TG T32GM07205 (JEM).

References

- Blumenfeld H. Impaired consciousness in epilepsy. *Lancet neurology*. 2012; 11:814–826.
- Blumenfeld H, McNally KA, Vanderhill SD, Paige AL, Chung R, Davis K, Norden AD, Stokking R, Studholme C, Novotny EJ Jr. et al. Positive and negative network correlations in temporal lobe epilepsy. *Cereb Cortex*. 2004a; 14:892–902. [PubMed: 15084494]
- Blumenfeld H, Rivera M, McNally KA, Davis K, Spencer DD, Spencer SS. Ictal neocortical slowing in temporal lobe epilepsy. *Neurology*. 2004b; 63:1015–1021. [PubMed: 15452292]
- Brashear HR, Zaborszky L, Heimer L. Distribution of gabaergic and cholinergic neurons in the rat diagonal band. *Neuroscience*. 1986; 17:439–451. [PubMed: 3517690]
- Braun AR, Balkin TJ, Wesenten NJ, Carson RE, Varga M, Baldwin P, Selbie S, Belenky G, Herscovitch P. Regional cerebral blood flow throughout the sleep-wake cycle. An H2(15)O PET study. *Brain*. 1997; 120(Pt 7):1173–1197. [PubMed: 9236630]
- Burmeister JJ, Gerhardt GA. Ceramic-based multisite microelectrode arrays for in vivo electrochemical recordings of glutamate and other neurochemicals. *TrAC Trends in Analytical Chemistry*. 2003; 22:498–502.
- Cunningham C, Chen WC, Shorten A, McClurkin M, Choezom T, Schmidt CP, Chu V, Bozik A, Best C, Chapman M, et al. Impaired consciousness in partial seizures is bimodally distributed. *Neurology*. 2014; 82:1736–1744. [PubMed: 24727311]
- Duque A, Tepper JM, Detari L, Ascoli GA, Zaborszky L. Morphological characterization of electrophysiologically and immunohistochemically identified basal forebrain cholinergic and neuropeptide Y-containing neurons. *Brain Structure and Function*. 2007; 212:55–73. [PubMed: 17717698]
- Englot DJ, Mishra AM, Mansuripur PK, Herman P, Hyder F, Blumenfeld H. Remote Effects of Focal Hippocampal Seizures on the Rat Neocortex. *The Journal of Neuroscience*. 2008; 28:9066–9081. [PubMed: 18768701]

- Englot DJ, Modi B, Mishra AM, DeSalvo M, Hyder F, Blumenfeld H. Cortical Deactivation Induced by Subcortical Network Dysfunction in Limbic Seizures. *The Journal of Neuroscience*. 2009; 29:13006–13018. [PubMed: 19828814]
- Englot DJ, Yang L, Hamid H, Danielson N, Bai X, Marfeo A, Yu L, Gordon A, Purcaro MJ, Motelow JE, et al. Impaired consciousness in temporal lobe seizures: role of cortical slow activity. *Brain*. 2010; 133:3764–3777. [PubMed: 21081551]
- Escueta AV, Kunze U, Waddell G, Boxley J, Nadel A. Lapse of consciousness and automatisms in temporal lobe epilepsy: a videotape analysis. *Neurology*. 1977; 27:144–155. [PubMed: 556830]
- Fox MD, Snyder AZ, Vincent JL, Corbetta M, Van Essen DC, Raichle ME. The human brain is intrinsically organized into dynamic, anticorrelated functional networks. *Proc Natl Acad Sci U S A*. 2005; 102:9673–9678. [PubMed: 15976020]
- Freund TF, Meskenaite V. gamma-Aminobutyric acid-containing basal forebrain neurons innervate inhibitory interneurons in the neocortex. *Proc Natl Acad Sci U S A*. 1992; 89:738–742. [PubMed: 1731348]
- Glenn LL, Steriade M. Discharge rate and excitability of cortically projecting intralaminar thalamic neurons during waking and sleep states. *The Journal of Neuroscience*. 1982; 2:1387–1404. [PubMed: 7119864]
- Gummadavelli A, Motelow JE, Smith N, Zahn Q, Schiff ND, Blumenfeld H. Thalamic stimulation to improve level of consciousness after seizures: Evaluation of electrophysiology and behavior. *Epilepsia*. (In press).
- Hallanger AE, Levey AI, Lee HJ, Rye DB, Wainer BH. The origins of cholinergic and other subcortical afferents to the thalamus in the rat. *The Journal of Comparative Neurology*. 1987; 262:105–124. [PubMed: 2442206]
- Hassani OK, Lee MG, Henny P, Jones BE. Discharge profiles of identified GABAergic in comparison to cholinergic and putative glutamatergic basal forebrain neurons across the sleep-wake cycle. *The Journal of neuroscience : the official journal of the Society for Neuroscience*. 2009; 29:11828–11840. [PubMed: 19776269]
- Heckers S, Geula C, Mesulam MM. Cholinergic innervation of the human thalamus: dual origin and differential nuclear distribution. *J Comp Neurol*. 1992; 325:68–82. [PubMed: 1282919]
- Hyde JS, Jesmanowicz A, Grist TM, Froncisz W, Kneeland JB. Quadrature detection surface coil. *Magnetic resonance in medicine : official journal of the Society of Magnetic Resonance in Medicine / Society of Magnetic Resonance in Medicine*. 1987; 4:179–184.
- Hyder F, Sanganahalli BG, Herman P, Coman D, Maandag NJ, Behar KL, Blumenfeld H, Rothman DL. Neurovascular and Neurometabolic Couplings in Dynamic Calibrated fMRI: Transient Oxidative Neuroenergetics for Block-Design and Event-Related Paradigms. *Frontiers in Neuroenergetics*. 2010; 2
- Kalmbach A, Hedrick T, Waters J. Selective optogenetic stimulation of cholinergic axons in neocortex. *Journal of Neurophysiology*. 2012; 107:2008–2019. [PubMed: 22236708]
- Kloster R, Engelskjøn T. Sudden unexpected death in epilepsy (SUDEP): a clinical perspective and a search for risk factors. *Journal of neurology, neurosurgery, and psychiatry*. 1999; 67:439–444.
- Langsjo JW, Alkire MT, Kaskinoro K, Hayama H, Maksimow A, Kaisti KK, Aalto S, Aantaa R, Jaaskelainen SK, Revonsuo A, Scheinin H. Returning from Oblivion: Imaging the Neural Core of Consciousness. *The Journal of neuroscience : the official journal of the Society for Neuroscience*. 2012; 32:4935–4943. [PubMed: 22492049]
- Lieb JP, Dasheiff RM, Engel J Jr. Role of the frontal lobes in the propagation of mesial temporal lobe seizures. *Epilepsia*. 1991; 32:822–837. [PubMed: 1743154]
- Marrosu F, Portas C, Mascia MS, Casu MA, Fa M, Giagheddu M, Imperato A, Gessa GL. Microdialysis measurement of cortical and hippocampal acetylcholine release during sleep-wake cycle in freely moving cats. *Brain Research*. 1995; 671:329–332. [PubMed: 7743225]
- McCormick DA. Cellular mechanisms underlying cholinergic and noradrenergic modulation of neuronal firing mode in the cat and guinea pig dorsal lateral geniculate nucleus. *The Journal of Neuroscience*. 1992; 12:278–289. [PubMed: 1309574]
- McCormick DA, Bal T. Sleep and arousal: thalamocortical mechanisms. *Annual review of neuroscience*. 1997; 20:185–215.

- McGinty D, Szymusiak R. Brain structures and mechanisms involved in the generation of NREM sleep: focus on the preoptic hypothalamus. *Sleep Medicine Reviews*. 2001; 5:323–342. [PubMed: 12530996]
- Mena-Segovia J, Sims HM, Magill PJ, Bolam JP. Cholinergic brainstem neurons modulate cortical gamma activity during slow oscillations. *The Journal of Physiology*. 2008; 586:2947–2960. [PubMed: 18440991]
- Mesulam M, Mufson EJ. Neural inputs into the nucleus basalis of the substantia innominata (Ch4) in the rhesus monkey. *Brain*. 1984; 107:253. [PubMed: 6538106]
- Mesulam M, Mufson EJ, Levey AI, Wainer BH. Cholinergic innervation of cortex by the basal forebrain: Cytochemistry and cortical connections of the septal area, diagonal band nuclei, nucleus basalis (Substantia innominata), and hypothalamus in the rhesus monkey. *The Journal of Comparative Neurology*. 1983a; 214:170–197. [PubMed: 6841683]
- Mesulam MM, Mufson EJ, Wainer BH, Levey AI. Central cholinergic pathways in the rat: an overview based on an alternative nomenclature (Ch1-Ch6). *Neuroscience*. 1983b; 10:1185–1201. [PubMed: 6320048]
- Metherate R, Ashe JH. Basal forebrain stimulation modifies auditory cortex responsiveness by an action at muscarinic receptors. *Brain Research*. 1991; 559:163–167. [PubMed: 1782557]
- Metherate R, Cox CL, Ashe JH. Cellular bases of neocortical activation: modulation of neural oscillations by the nucleus basalis and endogenous acetylcholine. *The Journal of Neuroscience*. 1992; 12:4701–4711. [PubMed: 1361197]
- Mishra AM, Ellens DJ, Schridde U, Motelow JE, Purcaro MJ, DeSalvo MN, Enev M, Sanganahalli BG, Hyder F, Blumenfeld H. Where fMRI and Electrophysiology Agree to Disagree: Corticothalamic and Striatal Activity Patterns in the WAG/Rij Rat. *The Journal of Neuroscience*. 2011; 31:15053–15064. [PubMed: 22016539]
- Moruzzi G, Magoun H. Brain Stem Reticular Formation and Activation of the EEG. *Electroencephalography and clinical neurophysiology*. 1949; 1:455–473. [PubMed: 18421835]
- Norden AD, Blumenfeld H. The role of subcortical structures in human epilepsy. *Epilepsy & Behavior*. 2002; 3:219–231. [PubMed: 12662601]
- Parikh V, Pomerieau F, Huettl P, Gerhardt GA, Sarter M, Bruno JP. Rapid assessment of vivo cholinergic transmission by amperometric detection of changes in extracellular choline levels. *European Journal of Neuroscience*. 2004; 20:1545–1554. [PubMed: 15355321]
- Paxinos, G.; Watson, C. *The Rat Brain: In Stereotaxic Coordinates*. 4th edn. Academic Press, Incorporated; 1998.
- Penfield W. Epileptic automatism and the centrencephalic integrating system. *Research publications - Association for Research in Nervous and Mental Disease*. 1952; 30:513–528. [PubMed: 12983687]
- Pinault D. A novel single-cell staining procedure performed in vivo under electrophysiological control: morpho-functional features of juxtacellularly labeled thalamic cells and other central neurons with biocytin or Neurobiotin. *Journal of Neuroscience Methods*. 1996; 65:113–136. [PubMed: 8740589]
- Posner, JB.; Saper, CB.; Schiff, ND.; Plum, F. *Plum and Posner's Diagnosis of Stupor and Coma*. Oxford University Press; USA: 2007.
- Poulet JFA, Fernandez LMJ, Crochet S, Petersen CCH. Thalamic control of cortical states. *Nature Neuroscience*. 2012; 15:370–372.
- Ros H, Sachdev RNS, Yu Y, Sestan N, McCormick DA. Neocortical Networks Entrain Neuronal Circuits in Cerebellar Cortex. *The Journal of Neuroscience*. 2009; 29:10309–10320. [PubMed: 19692605]
- Rye DB, Wainer BH, Mesulam MM, Mufson EJ, Saper CB. Cortical projections arising from the basal forebrain: A study of cholinergic and noncholinergic components employing combined retrograde tracing and immunohistochemical localization of choline acetyltransferase. *Neuroscience*. 1984; 13:627–643. [PubMed: 6527769]
- Saper CB, Fuller PM, Pedersen NP, Lu J, Scammell TE. Sleep State Switching. *Neuron*. 2010; 68:1023–1042. [PubMed: 21172606]

- Saper CB, Scammell TE, Lu J. Hypothalamic regulation of sleep and circadian rhythms. *Nature*. 2005; 437:1257–1263. [PubMed: 16251950]
- Schridde U, Khubchandani M, Motelow JE, Sanganahalli BG, Hyder F, Blumenfeld H. Negative BOLD with Large Increases in Neuronal Activity. *Cerebral Cortex*. 2008; 18:1814–1827. [PubMed: 18063563]
- Scoville WB, Milner B. Loss of recent memory after bilateral hippocampal lesions. *Journal of Neurology, Neurosurgery & Psychiatry*. 1957; 20:11–21.
- Semba K, Fibiger HC. Afferent connections of the laterodorsal and the pedunclopontine tegmental nuclei in the rat: A retro- and antero-grade transport and immunohistochemical study. *The Journal of Comparative Neurology*. 1992; 323:387–410. [PubMed: 1281170]
- Sperling MR. The consequences of uncontrolled epilepsy. *CNS spectrums*. 2004; 9:98–101. 106–109. [PubMed: 14999166]
- Steriade M. Acetylcholine systems and rhythmic activities during the waking-sleep cycle. In *Progress in brain research* (Elsevier). 2004:179–196.
- Steriade M, Amzica F, Nuñez A. Cholinergic and noradrenergic modulation of the slow (approximately 0.3 Hz) oscillation in neocortical cells. *Journal of Neurophysiology*. 1993a; 70:1385–1400. [PubMed: 8283204]
- Steriade M, Nuñez A, Amzica F. A novel slow (< 1 Hz) oscillation of neocortical neurons in vivo: depolarizing and hyperpolarizing components. *The Journal of Neuroscience*. 1993b; 13:3252–3265. [PubMed: 8340806]
- Sterman MB, Clemente CD. Forebrain inhibitory mechanisms: cortical synchronization induced by basal forebrain stimulation. *Exp Neurol*. 1962; 6:91–102. [PubMed: 13916975]
- Ushimaru M, Ueta Y, Kawaguchi Y. Differentiated participation of thalamocortical subnetworks in slow/spindle waves and desynchronization. *The Journal of Neuroscience*. 2012; 32:1730–1746. [PubMed: 22302813]
- Varoqueaux F, Poulain P. Projections of the mediolateral part of the lateral septum to the hypothalamus, revealed by Fos expression and axonal tracing in rats. *Anatomy and embryology*. 1999; 199:249–263. [PubMed: 10068091]
- Wang H, Morales M. Pedunclopontine and laterodorsal tegmental nuclei contain distinct populations of cholinergic, glutamatergic and GABAergic neurons in the rat. *European Journal of Neuroscience*. 2009; 29:340–358. [PubMed: 19200238]
- Williams JA, Comisarow J, Day J, Fibiger HC, Reiner PB. State-dependent release of acetylcholine in rat thalamus measured by in vivo microdialysis. *The Journal of Neuroscience*. 1994; 14:5236–5242. [PubMed: 8083733]
- Young GB. The EEG in coma. *J Clin Neurophysiol*. 2000; 17:473–485. [PubMed: 11085551]
- Zhang H, Lin SC, Nicolelis MA. Acquiring local field potential information from amperometric neurochemical recordings. *J Neurosci Methods*. 2009; 179:191–200. [PubMed: 19428527]

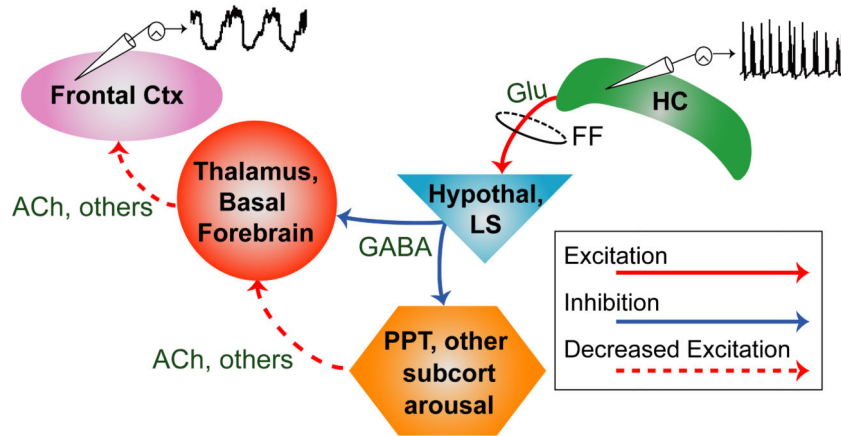


Figure 1.

Network inhibition hypothesis and predictions.

Prediction 1: Seizure activity in the hippocampus (HC) propagates (via fimbria-fornix, FF and other pathways) to increase activity in inhibitory and sleep-promoting regions such as the anterior hypothalamus (Hypothal) and lateral septum (LS); as a consequence, subcortical arousal systems including the thalamus, basal forebrain, pedunculopontine tegmental nucleus (PPT), and other subcortical arousal systems show depressed activity. Prediction 2: Firing of identified arousal neurons, such as cholinergic neurons in PPT and basal forebrain, decreases during seizures. Prediction 3: Release of arousal neurotransmitters including acetylcholine (ACh) is decreased in both thalamus and cortex (Ctx). This in turn leads to decreased cortical arousal and slow-waves in the cortex.

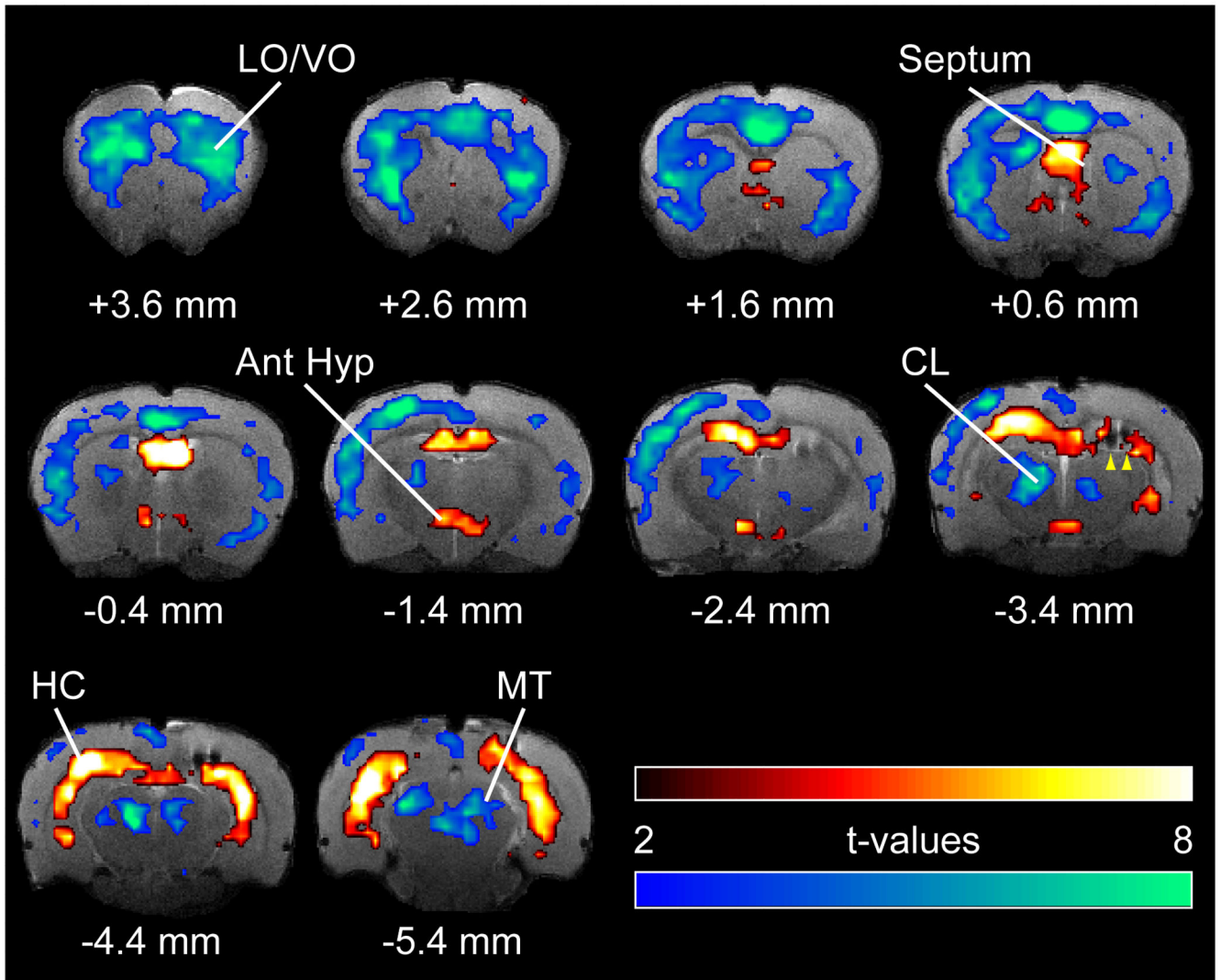


Figure 2.

Hippocampal, cortical and subcortical BOLD fMRI changes during limbic seizures. T-map of ictal changes during partial seizures (from 30s pre-seizure baseline) reveals complicated network of changes. Widespread cortical decreases are accompanied by mixed subcortical increases and decreases. Increases are seen in known areas of seizure propagation such as the hippocampus (HC) and lateral septum as well as in sleep promoting regions such as the anterior hypothalamus (Ant Hyp). Decreases are seen in the cortex, most prominently in lateral and ventral orbital frontal cortex (LO/VO) and in medial regions including cingulate and retrosplenial cortex. Decreases are also seen in arousal promoting regions such as the thalamic intralaminar nuclei including centrolateral nucleus (CL), as well as in the midbrain tegmentum (MT). The arrowheads at AP -3.4 mm signify the hippocampal electrode artifact. Warm colors represent fMRI increases, and cool colors represent decreases, superimposed on coronal anatomical images from the template animal. AP coordinates in millimeters relative to bregma (Paxinos and Watson, 1998). 10 animals, with FDR corrected threshold $P < 0.05$. See also Figure S1

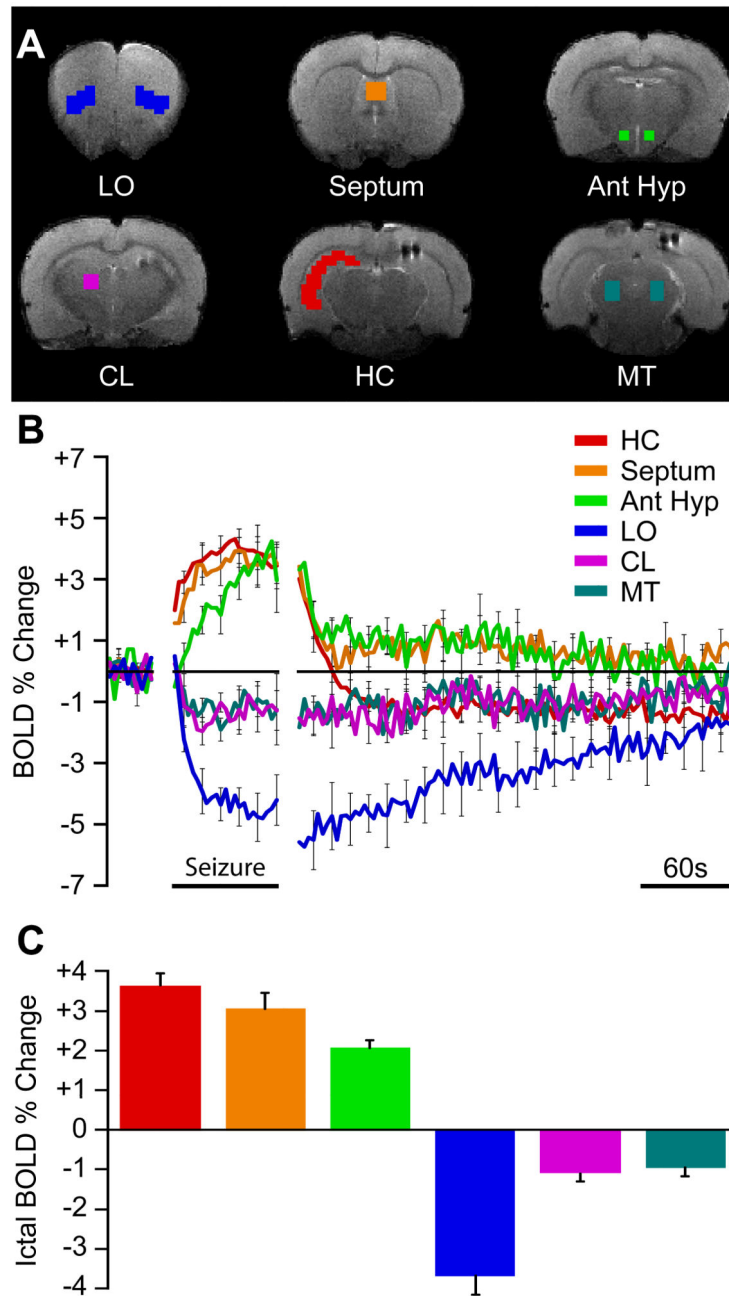


Figure 3. BOLD region of interest (ROI) time courses reveal increases and decreases during seizures and eventual return to baseline.

(A) Example regions of interest on anatomical brain images.

(B) Mean ROI time courses (\pm SEM) for data 30 seconds prior to seizure onset, seizure timecourse scaled to mean seizure duration, and unscaled postictal timecourse aligned to seizure end.

(C) Mean ictal BOLD change is increased in limbic and sleep promoting regions and decreased in cortical and arousal regions. Error bars are SEM. All changes during seizures

were significantly different from baseline (1-sample t-tests Holm-Bonferroni corrected, $P < 0.05$). Data are from same animals and seizures as in Figure 2. Ant Hyp, anterior hypothalamus; HC, hippocampus; LO, lateral orbital frontal cortex; CL, central lateral (intralaminar) thalamus; MT, midbrain tegmentum; Septum, lateral septal nuclei. See also Figure S1

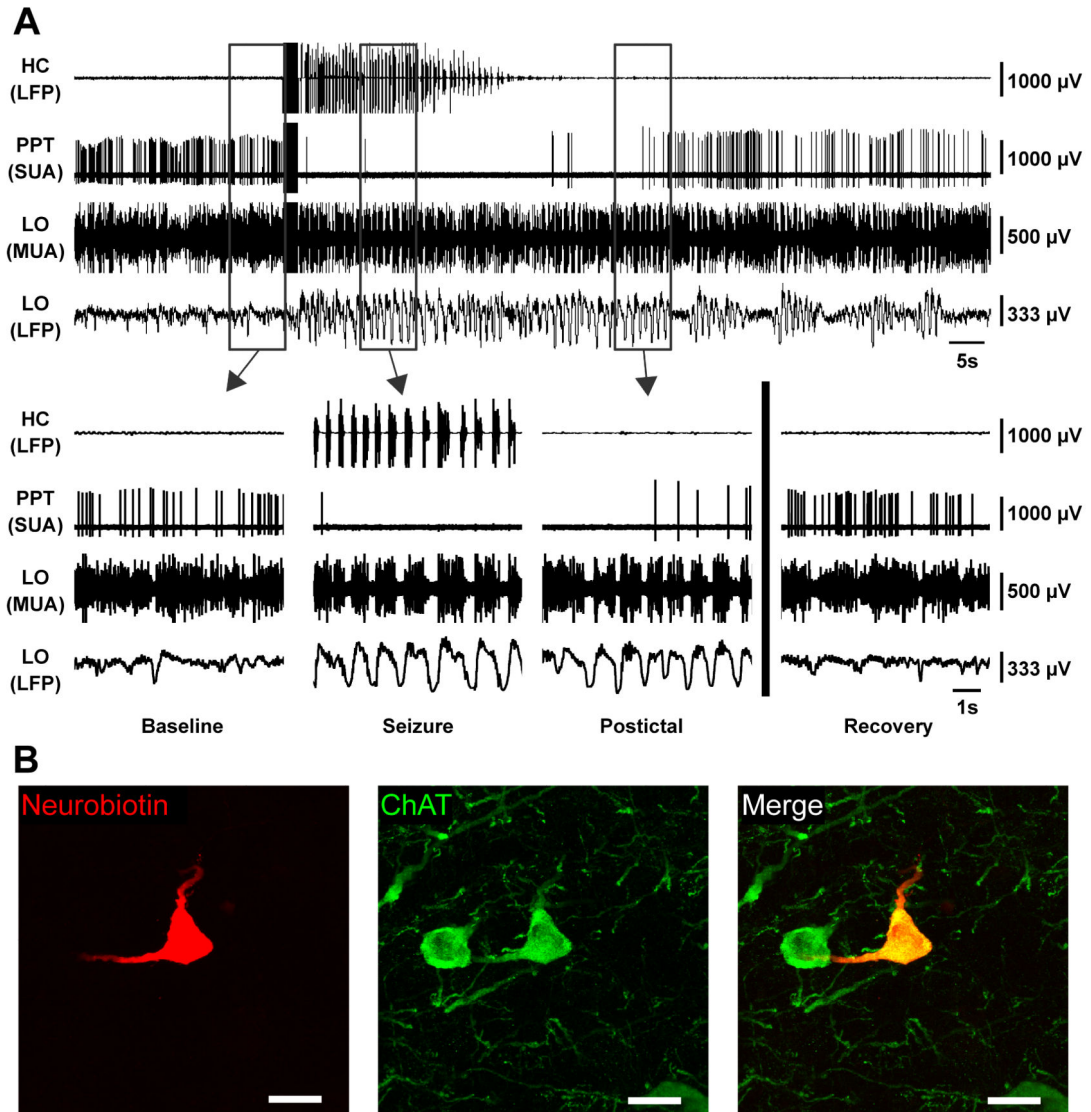


Figure 4.

Brainstem cholinergic neuron ceases firing during partial seizure.

(A) Cholinergic neuron in PPT dramatically decreases firing during seizure activity.

Expanded segments of baseline, seizure, and postictal recordings from the boxed regions in (A) as well as a recovery period 7 minutes after the stimulus.

(B) Labeled cholinergic cell recorded in (A) stained for Neurobiotin in left panel, choline acetyltransferase (ChAT) in middle panel, and merge in right panel. Scale bars are 20 micrometers. HC, hippocampus; PPT, pedunculopontine tegmental nucleus; LO, lateral orbitofrontal cortex; LFP, local field potential; SUA, single unit (juxtacellular) activity; MUA, multiunit activity. See also Figures S2

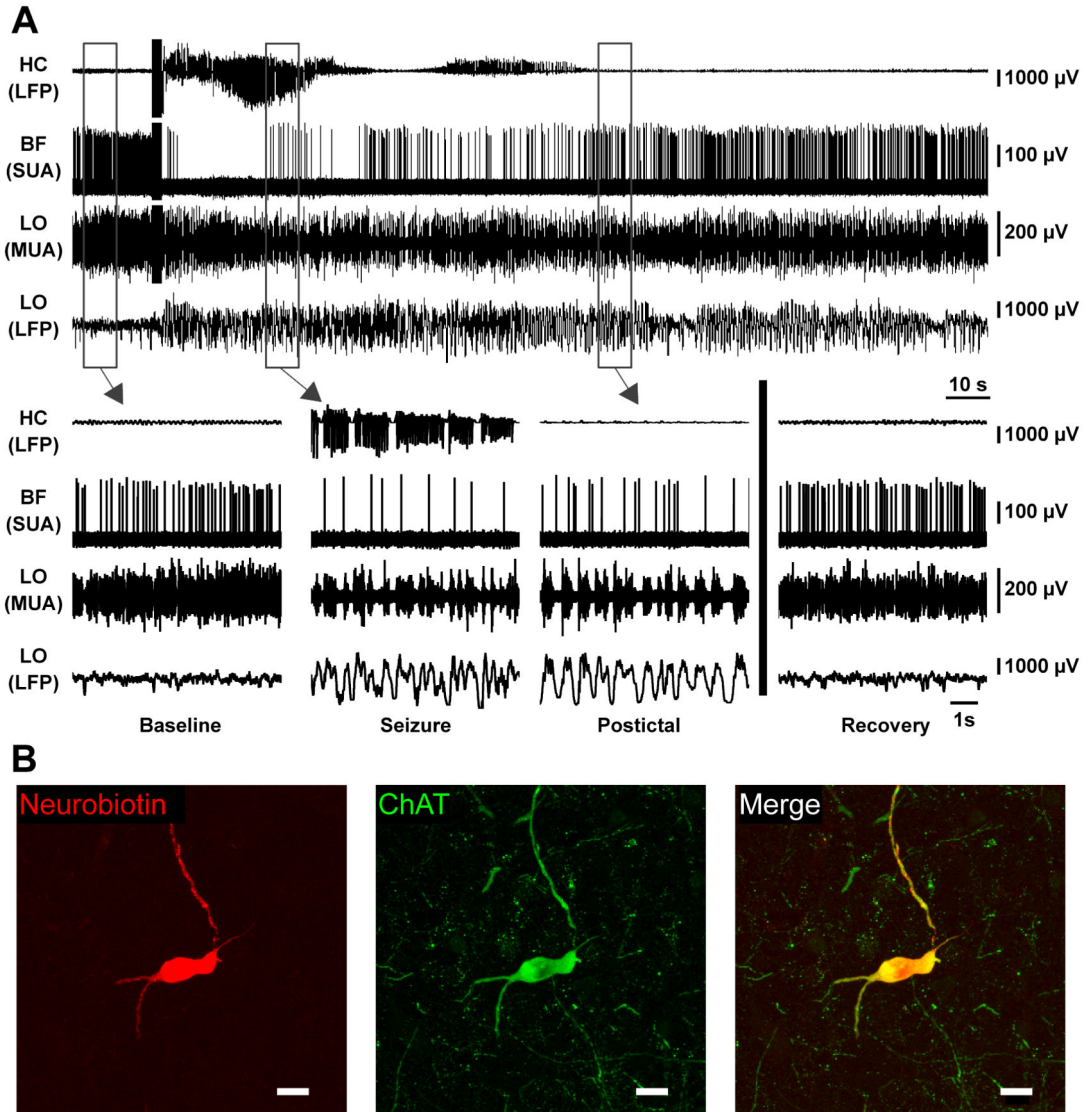


Figure 5.

Basal forebrain cholinergic neuron decreases firing during partial seizure.

(A) Cholinergic neuron in basal forebrain dramatically decreases firing during seizure activity. Expanded segments of baseline, seizure, and postictal recordings from the boxed regions in (A) as well as a recovery period 4.5 minutes after the stimulus.

(B) Labeled cholinergic cell recorded in (A) stained for Neurobiotin in left panel, choline acetyltransferase (ChAT) in middle panel, and merge in right panel. Scale bars are 20 micrometers. HC, hippocampus; BF, basal forebrain; LO, lateral orbitofrontal cortex; LFP, local field potential; SUA, single unit (juxtacellular) activity; MUA, multiunit activity. See also Figure S5

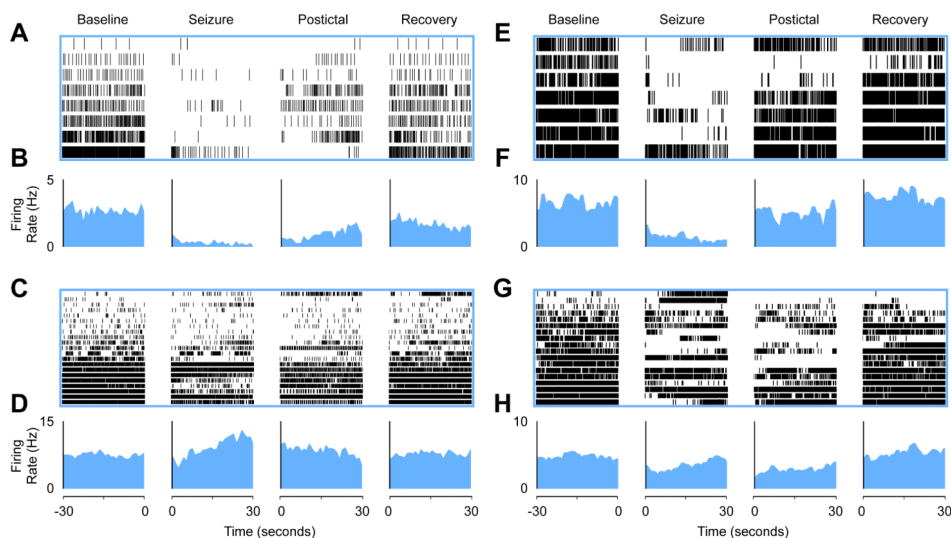


Figure 6.

Cholinergic neurons in PPT and basal forebrain decrease firing during partial seizures while firing of non-cholinergic nearby neurons is mixed.

(A and B) Partial seizures suppressed firing in PPT cholinergic neurons during seizures.

(A) Raster plot (8 cells from 8 animals) and (B) mean firing rate histogram data.

(C and D) PPT non-cholinergic neurons have a variable firing rate during seizures. Mean firing rate during seizures. (C) Raster (21 cells from 19 animals) and (D) mean firing rate histogram data.

(E and F) Partial seizures suppressed firing in basal forebrain cholinergic neurons during seizures. (E) Raster (7 cells from 6 animals) and (F) mean firing rate histogram data.

(G and H) BF non-cholinergic neurons have a variable firing rate during seizures. (G) Raster (18 cells from 12 animals) and (H) mean firing rate histogram data. Although selected 30 second segments are displayed here, the entire timecourses of mean firing are shown in Figure S7. Statistics were performed on the entire seizure period vs. baseline for all experiments. Baseline is 30 seconds prior to seizure onset. Seizure is the first 30 seconds following seizure onset. Postictal is the first 30 seconds following seizure end. Recovery is the last 30 seconds before either the animal was re-anesthetized or the neuron was labeled by the juxtacellular method. Neurons in raster plots (A, C, E, and G) are ordered based on baseline firing rate for visualization. Firing rates (B, D, F, H) are binned by 1 second. See also Figures S2, S3, S4, S5, S6, and S7.

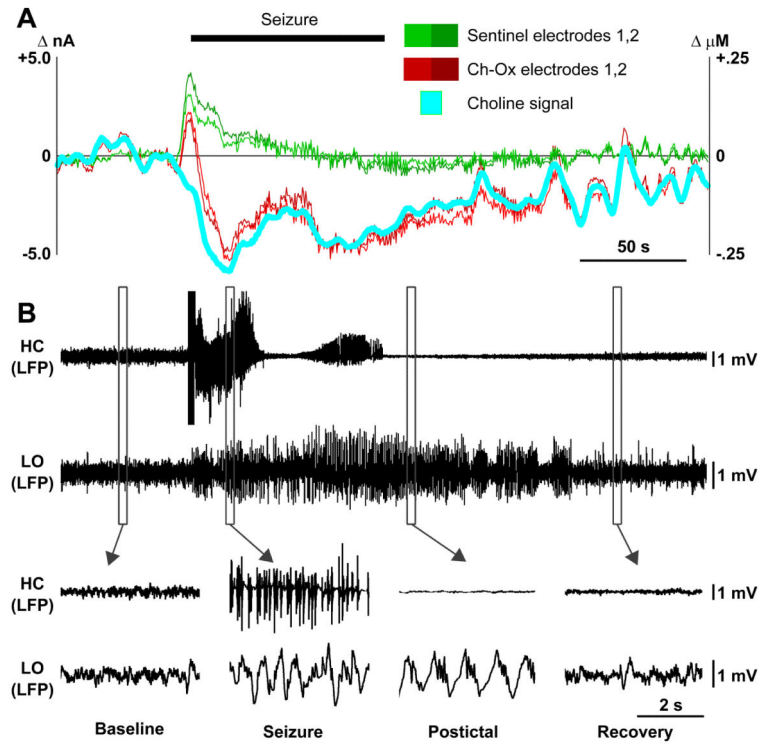


Figure 7.

Decreased cortical choline accompanies cortical slow-waves during partial limbic seizure. (A) Amperometric choline recordings in the cortex during partial seizure. Cyan represents the choline signal obtained by subtracting mean signal from two sentinel electrodes (Green 1,2) from mean of the two choline oxidase-coated electrodes (Red, Ch-Ox 1,2). Current is on left axis, and choline concentration on right axis obtained by *in vitro* choline calibration for each electrode (see also Figure S8).

(B) Simultaneous recording of partial seizure. Local field potential (LFP) signals from both hippocampus (HC) and lateral orbital frontal cortex (LO) are shown. Hippocampal seizures elicit slow oscillations in the cortex that persist postictally before recovering back to baseline (lower insets).

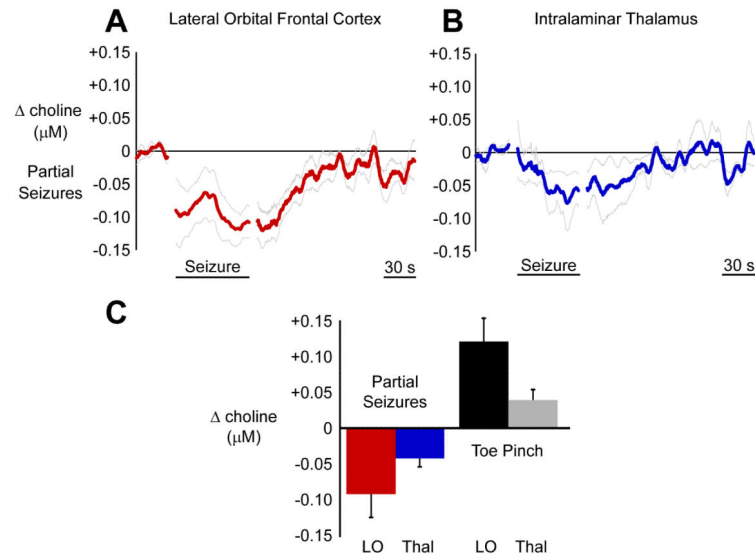


Figure 8.

Choline signal decreases in the cortex and the thalamus during partial seizures.

(A) In the cortex, choline recordings decrease during partial seizures with gradual recovery during the postictal and recovery periods.

(B) The pattern is the same in the thalamus. Choline recordings decrease during partial seizures.

(C) Mean ictal changes in the cortex and the thalamus relative to 30 s baseline are shown along with mean changes during toe pinch to provide a common physiological change for comparison. Choline decreases in partial seizures were all statistically significant (paired t-tests Holm-Bonferroni corrected, $P < 0.05$). Toe pinch also elicited significant choline increases in cortex and thalamus (paired t-tests Holm-Bonferroni corrected, $P < 0.05$). Error bars in A-C are SEM. Mean timecourses in A and B are data 30 seconds prior to seizure onset, seizure timecourse scaled to mean seizure duration, and unscaled postictal timecourse aligned to seizure end. LO, lateral orbitofrontal cortex; Thal, intralaminar thalamus.